Broadband measurement of rate-dependent viscoelasticity at nanoscale using scanning probe microscope: Poly(dimethylsiloxane) example

Zhonghua Xu, Kyongsoo Kim, Qingze Zou, and Pranav Shrotriya

Citation: Applied Physics Letters **93**, 133103 (2008); doi: 10.1063/1.2990759
View online: http://dx.doi.org/10.1063/1.2990759
View Table of Contents: http://scitation.aip.org/content/aip/journal/apl/93/13?ver=pdfcov
Published by the AIP Publishing

Broadband measurement of rate-dependent viscoelasticity at nanoscale using scanning probe microscope: Poly(dimethylsiloxane) example

Zhonghua Xu, Kyongsoo Kim, Qingze Zou,[a] and Pranav Shrotriya
Department of Mechanical Engineering, Iowa State University, Ames, Iowa 50011, USA

(Received 6 August 2008; accepted 8 September 2008; published online 29 September 2008)

A control approach to achieve nanoscale broadband viscoelastic measurement using scanning probe microscope (SPM) is reported. Current SPM-based force measurement is too slow to measure rate-dependent phenomena, and large (temporal) measurement errors can be generated when the sample itself changes rapidly. The recently developed model-less inversion-based iterative control technique is used to eliminate the dynamics and hysteresis effects of the SPM hardware on the measurements, enabling rapid excitation and measurement of rate-dependent material properties. The approach is illustrated by the mechanical characterization of poly(dimethylsiloxane) over a broad frequency range of three orders of magnitude (~1 Hz to 4.5 KHz). © *2008 American Institute of Physics*. [DOI: 10.1063/1.2990759]

Scanning probe microscope (SPM) has become an enabling tool to quantitatively measure the mechanical properties of a wide variety of materials, particularly the rate-dependent viscoelasticity of soft materials such as live cells.[1] However, current nanoscale viscoelasticity measurement is time consuming and limited to the narrow band of low frequency range. For example, in the force-modulation measurement[2] where a sinusoidal force signal (i.e., ac signal) of small amplitude is augmented to the constant-rate input signal and applied to drive the cantilever, the modulation frequency is limited to relatively low frequency range (a couple of hundreds of hertz) and the modulation amplitude is small (several tens of nanometers). Rapid broadband viscoelasticity measurement is needed to measure rate-dependent phenomena,[3] particularly when dynamic evolution of the sample is of interest.[4] The low speed of SPM is because at high speeds, the SPM measurement of material response can suffer from large uncertainties due to the convolution of adverse effects such as hysteresis and dynamics of the piezoactuator, dynamics of the probe, the mechanical mounting, etc., into the measured data.

We report a control approach to characterize broadband viscoelasticity based on the concept of system identification, i.e., the system dynamics (e.g., the broadband viscoelasticity) can be identified by exciting the system with an appropriate input (which satisfies the persistent excitation condition[5]) and measuring the corresponding output response. The challenge, however, is to eliminate the adverse effects coupled into the measured data. In the proposed method, we use the recently developed model-less inversion-based iterative control (MIIC) technique[6,7] to eliminate these adverse effects in the measurement. Thus, the time-consuming demodulation process involved in the force-modulation method is avoided. Instead, desired excitation force of rich frequencies can be exerted onto the soft material (through the SPM probe), and the corresponding mechanical response of the soft material (the indentation) can be accurately measured. Specifically, a band-limited white-noise type of excitation force is used, and to determine the indentation on the soft material, the same control input is also applied to the force measurement on a hard reference material, and the cantilever deflections measured from these two measurements are compared. Then the force-indentation data can be used in a contact mechanics model to compute the rate-dependent compliance of the soft sample. Compared to existing viscoelasticity measurement methods at nanoscale as well as at microscale to bulk scales[8] (the microscale/bulk scale methods are also oscillatory based and rely on optical detection—thus their resolution is limited by the light wavelength), the proposed approach is fundamentally different in the use of advanced control techniques to eliminate the convolution of the hardware dynamics into the measurement, as well as to attain rapid excitation of the mechanical behavior of materials. As a result, the proposed approach can achieve nanoscale (local) quantification of material viscoelasticity over a larger frequency range with shorter amount of time (on the same hardware platform).

The basic idea of the MIIC control technique[6,7] is to "learn" the system's adverse effects (hysteresis and dynamics) by iteratively updating the control input with the output measured from the previous trial (see Fig. 1). The MIIC algorithm can be described in frequency domain as

$$u_0(j\omega) = \alpha z_d(j\omega), \quad k = 0,$$

$$u_k(j\omega) = \begin{cases} \dfrac{u_{k-1}(j\omega)}{z_{k-1}(j\omega)} z_d(j\omega), & \text{when } z_{k-1}(j\omega) \neq 0, \\ & \text{and } k \geqslant 1, \\ 0 & \text{otherwise} \end{cases} \tag{1}$$

where $f(j\omega)$ is the Fourier transform of the signal $f(t)$, $z_d(\cdot)$ is the desired output trajectory, $z_k(\cdot)$ is the system output for the input $u_k(\cdot)$ applied during the kth iteration, and $\alpha \neq 0$ is a prechosen constant. In implementations, distur-

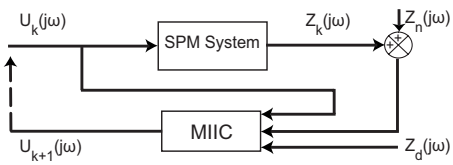

FIG. 1. The system diagram of the MIIC algorithm.

[a]Author to whom correspondence should be addressed. Electronic mail: qzzou@iastate.edu.

bance and measurement noise exist, the system output becomes $\hat{z}_k(j\omega)=z_k(j\omega)+z_n(j\omega)$, where $z_k(j\omega)$ denotes the linear part of the system response, i.e., $z_k(j\omega)=G(j\omega)u_k(j\omega)$, and $z_n(j\omega)$ denotes the disturbance (and/or measurement noise, Fig. 1). Then it has been shown in Ref. 6 that if the bound of the following noise/disturbance to (desired) signal ratio (NSR) at frequency ω, $\epsilon(\omega)$, is less than $1-\sqrt{2}/2$, i.e., $|z_n(j\omega)|/|z_d(j\omega)| \leqslant \epsilon(\omega) < [1-(\sqrt{2}/2)]$, $\forall k$, the output tracking can be improved by using the MIIC algorithm,

$$\lim_{x\to\infty}\left|\frac{z_k(j\omega)-z_d(j\omega)}{z_d(j\omega)}\right| \leqslant \frac{2[1-\epsilon(\omega)]}{1-2\epsilon(\omega)}\epsilon(\omega) < 1. \qquad (2)$$

The above Eq. (2) shows that precision tracking of the desired trajectory over a broad frequency range can be achieved provided that the NSR $\epsilon(\omega)$ is small in that frequency range. Such a "trackable" frequency range can be significantly larger than the open-loop bandwidth of the system.[6]

The efficacy of the iterative control approaches to eliminate the hardware dynamics effects on SPM force measurement has been demonstrated in the authors' recent work.[9] This article extends such efforts by improving both the iterative control algorithm (the SPM dynamics model is needed by the control algorithm in Ref. 9) and more importantly, the excitation force profile (the band-limited white noise rather than the quasistatic triangle signal[9]). Thus, the contribution of this article is the utilization of the MIIC technique[6,7] to enable broadband nanomechanical measurements and arrive at quantitative characterization of the viscoelasticity of materials.

The proposed approach was used to measure the rate-dependent viscoelasticity of poly(dimethylsiloxane) (PDMS) on a commercial SPM system (Dimension 3100, Veeco Inc.). The SPM controller was customized so the external control input bypassed the PID control circuit when the input was sent to drive the vertical z-axis piezoactuator directly. The cantilever deflection sensor signal was acquired through a data acquisition (DAQ) card and MATLAB-xPC-target software package was used to implement the MIIC algorithm through the DAQ card and process the data. First, the MIIC algorithm was applied to enable the cantilever deflection on a PDMS sample to track a band-limited white-noise desired trajectory (see Ref. 9 for the preparation of the PDMS sample). This tracking implied that the adverse effects of the z-axis SPM dynamics were eliminated to allow the desired excitation force profile to be exerted onto the PDMS sample. The cutoff frequency of the band-limited white noise (with duration of 6 s) was chosen at 4.5 KHz (the open-loop z-axis SPM dynamics, from the piezoactuator to the cantilever, has one dominant resonant peak at ~3.7 KHz). Then this trajectory was cascaded with two copies of its own and then used as the desired trajectory in the MIIC algorithm. The tracking error was very small (the RMS error was <4%). Next, the converged iterative control input was applied along with a small normal force for the PDMS sample, and the cantilever deflection was measured. The small normal load was added to avoid the pull-off of the probe from the sample during the measurements. Finally, the same control input was applied when the sample was replaced with a hard reference sample (sapphire) and the deflection signal was measured.

The experimentally measured cantilever displacements for the PDMS sample and the sapphire sample are compared

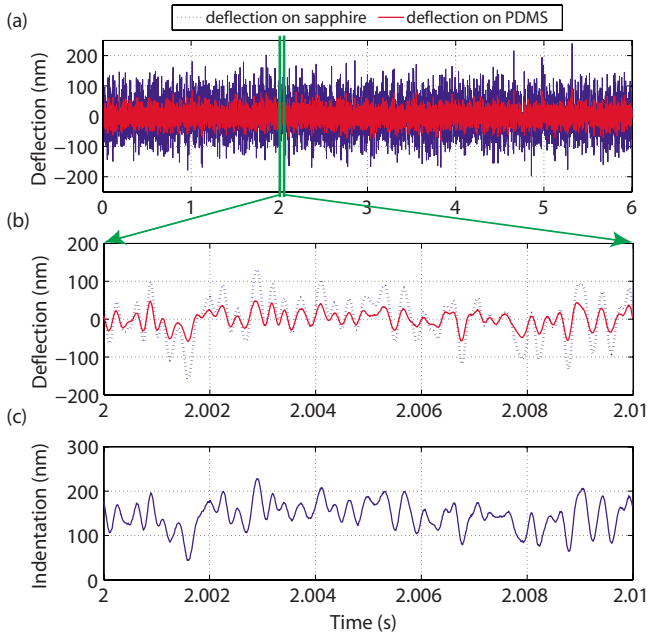

FIG. 2. (Color online) (a) The comparison of the experimentally measured deflection signals on the PDMS sample and that on the sapphire sample, (b) the zoomed-in view of plot (a) for time $t \in [2, 2.01]$ s, and (c) the difference between these two deflection signals within the zoomed-in interval.

in Fig. 2, where Fig. 2(a) is for the entire 6 s period and Fig. 2(b) presents the zoomed-in view of Fig. 2(a) for an interval of 0.01 s. The cantilever sensitivity constant (85 nm/V, experimentally calibrated as in Ref. 10) relating deflection to displacement was used. The indentation on the PDMS sample by the excitation force was obtained from the difference of the two cantilever displacement signals, as shown in Fig. 2(c) for the zoomed-in interval $t \in [2, 2.01]$ s. Finally, the cantilever deflection measured on the PDMS sample was converted to the excitation force exerted on the PDMS sample by using the cantilever spring constant (0.065 N/m, calibrated by using the thermal noise method Ref. 10). The magnitude of the frequency components of the excitation force and that of the indentation are plotted in Figs. 3(a) and 3(b), respectively.

Figure 3 shows that the excitation force has the band-limited white-noise characteristics—the force signal contained rich frequency components of similar amplitude uniformly distributed across the entire frequency spectrum (from ~1 Hz to 4.5 KHz). Thus, such an applied force can sufficiently excite the broadband material response. Moreover, the cantilever deflection obtained on the sapphire sample was always larger than that on the PDMS sample [see Figs. 2(b) and 2(c)]. The larger deflection occurred because the elastic modulus of sapphire is much higher (over five

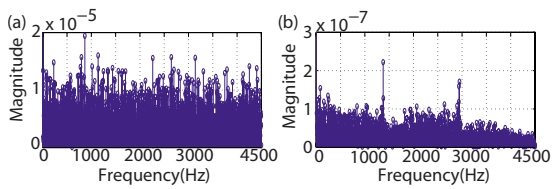

FIG. 3. (Color online) (a) The magnitude of the frequency components in the tip-sample interaction force showing the band-limited white-noise characteristic and (b) the magnitude of the frequency components in the indentation into the PDMS under the force of (a).

orders of magnitude higher) than that of PDMS. The experimental results also reveal the *frequency dependence* of the indentation response of PDMS: as frequency was increased, the magnitude of the frequency components in the obtained indentation tended to become smaller [Fig. 3(b)], even though the counterpart in the excitation force was maintained across the frequency spectrum [Fig. 3(a)]. Such a trend clearly demonstrated the rate-dependent mechanical response of PDMS: as the excitation frequency was increased, PDMS became stiffer, which can be due to viscoelastic nature of the polymer; hence, a faster external deformation rate transitioned the response of PDMS from rubbery toward being glassy.[9] These experiment results demonstrate the efficacy of the proposed technique.

Finally, the measured force-indentation data were used to compute the complex compliance of the PDMS sample based on the following classical Hertz contact model,[1] $h^{3/2}(t)=\mathcal{C}_1\int_0^t J(t-\tau)[dP(\tau)/d\tau]d\tau$, where $P(t)$ is the interaction force between the tip and the sample surface, $h(t)$ is the indentation of the tip on the sample surface, $J(t)$ is the creep compliance functional of the sample material in uniaxial compression, and the constant $\mathcal{C}_1$ is given as $\mathcal{C}_1=[3(1-\nu^2)]/(4\sqrt{R})$, with R and ν being the radius of the tip and the Poisson ratio of the soft sample, respectively. Note that the assumptions underlying the above analysis–the friction and adhesion force during indentation are negligible–were valid for these experiments, because the horizontal in-plane displacement of the cantilever relative to the sample was negligible and the probe was in continuous contact with the sample throughout the measurements. The probe radius of 57 nm was experimentally characterized through imaging a standard probe calibration sample (porous aluminum PA01).[10] The complex compliance $J(j\omega)$ is then computed by using the Hertz contact model. Then the obtained complex compliance $J(j\omega)$ was modeled by using a fourth-order Prony series, $J(j\omega)=J_0/(j\omega)-\Sigma_{i=1}^4(J_i/(j\omega+1/\tau_i))$, where the fully relaxed coefficient J_0, the compliance coefficients J_i, and the retardation times τ_i were estimated via curve fitting using MATLAB. The obtained parameters are: $J_0=9.11\times10^{-6}$ Pa^{-1}, $J_i=(-2.08,-1.53,-1.51,-2.37)\times10^{-6}$ Pa^{-1}, and $\tau_i=(25.28,2.90,0.47,0.05)$ ms, for $i=1$, 2, 3, and 4. The measured creep compliance of PDMS sample is plotted in Fig. 4 for time $t\in[1/4.5\ \mathrm{ms},6\ \mathrm{s}]$ (where the starting time instant 1/4.5 ms corresponds to the upper bound of the measured frequency 4.5 KHz). According to calculated creep compliance, the instantaneous modulus of PDMS is about 1.33 MPa and it quickly relaxes to 0.2 MPa. Magnitudes of instantaneous and fully relaxed modulus compare well with DMA tests on the same samples.[9] At room temperature, PDMS is above its glass temperature and displays a clear viscoelastic solid response. Our proposed characterization technique clearly captures the rate dependent viscoelastic nature of the PDMS polymer. These results demonstrate the efficacy of our technique for rapid broadband viscoelastic characterization.

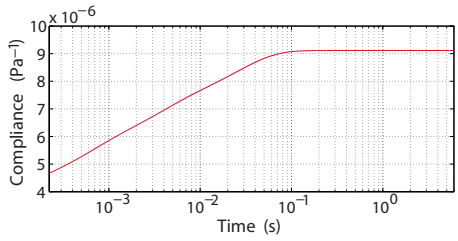

FIG. 4. (Color online) The creep complex compliance of PDMS plotted in logarithmic scale for time $t\in[1/4.5\ \mathrm{ms},6\ \mathrm{s}]$.

The authors would like to thank Professors. Sriram Sundararajan and Zhiqun Lin (both from Iowa State University) for their help in characterizing the SPM probe and preparing the PDMS sample, respectively. The financial support of NSF under Grant Nos. CMMI-0626417 and DUE-0632908 are gratefully acknowledged.

[1] H.-J. Butt, B. Cappella, and M. Kappl, Surf. Sci. Rep. **59**, 1 (2005).
[2] S. A. S. Asif, K. J. Wahl, and R. J. Colton, Rev. Sci. Instrum. **70**, 2408 (1999).
[3] E. Lupton, C. Nonnenberg, I. Frank, F. Achenbach, J. Weis, and C. Bräuchle, Chem. Phys. **414**, 132 (2005).
[4] G. T. Charras and M. A. Horton, Biophys. J. **83**, 858 (2002).
[5] L. Ljung, *System Identification: Theory for the User*, 2nd ed. (Prentice-Hall, Englewood Cliffs, NJ, 1999), Chaps. 2 and 6
[6] K.-S. Kim and Q. Zou, Proceedings of the American Control Conference, Seattle, WA, 2008 (IEEE), pp. 2210–2215.
[7] Y. Li and J. Bechhoefer, Proceedings of the American Control Conference, Seattle, WA, 2008 (IEEE), pp. 2703–2709.
[8] M. Gardel, M. Valentine, and D. Weitz, *Microscale Diagnostic Techniques* (Springer, Berlin, 2005), Chap. 1.
[9] K. Kim, Z. Lin, P. Shriotrya, S. Sundararajan, and Q. Zou, Ultramicroscopy **108**, 911 (2008).
[10] J. L. Hutter and J. Bechhoefer, Rev. Sci. Instrum. **64**, 1868 (1993).